J Surfact Deterg (2017) 20:1453–1465
DOI 10.1007/s11743-017-2026-9

ORIGINAL ARTICLE

Self-Aggregation and Emulsifying Properties of Methyl Ester Sulfonate Surfactants

Amel Asselah[1,2] · Aurora Pinazo[3] · Amalia Mezei[3] · Lourdes Pérez[3] · Amel Tazerouti[1]

Received: 16 February 2017 / Accepted: 25 September 2017 / Published online: 9 October 2017

Abstract Methyl ester sulfonate (MES) anionic surfactants made from natural resources are of particular interest as sustainable surfactants. They offer good physicochemical properties for applications as detergents and emulsifiers. The liquid crystal structures of MES surfactants synthesized in a previous work were determined by polarizing optical microscopy (POM) and small-angle X-ray scattering (SAXS). The emulsifying activity for each surfactant was also measured, and the stability of emulsions was estimated and compared to that induced by sodium dodecyl sulfate (SDS). The POM micrographs showed the presence of birefringent textures. Several factors, including temperature and hydration, influenced the stability of the phases and their structure. SAXS confirmed the structure of the phases formed by dry and hydrated ϕ-MES surfactants at 25 °C, giving the position of peaks corresponding to the ratio 1:2:3 and revealing the phase transitions of lamellar to double lamellar or the reverse. Also, the Bragg distance (*d*) decreased with an increase in chain length from 13 to 17 carbon atoms and an increase in the area per molecule of surfactant. The geometric packing parameters were also determined, and suggest that surfactants are tilted. The stability of surfactant emulsions is around 60%, which is comparable to that of SDS. The micrographs show that the emulsions formed are O/W, and an increase in chain length gives rise to a decrease in the size of the emulsion droplets. These results are confirmed by the values of hydrophilic-lipophilic balance (HLB) which reveals the hydrophilic nature of these surfactants.

Keywords Fatty acids · Methyl ester sulfonates · Aggregation · Liquid crystals · Birefringence · Emulsification

✉ Amel Asselah
asselah.amel@yahoo.fr; aasselah@usthb.dz

[1] Laboratoire de Chimie Organique Appliquée, Faculté de Chimie, Université des Sciences et de la Technologie Houari Boumediene (USTHB), Bab Ezzouar 16111, Algiers, Algeria

[2] Département du Génie des Procédés, Faculté des Sciences de l'Ingénieur (FSI), Université M'Hamed Bougara de Boumerdes (UMBB), Avenue de l'Indépendance, 35000 Boumerdes, Algeria

[3] Institut de Química Avançada de Catalunya, IQAC-CSIC, c/Jordi Girona 18-26, 08034 Barcelona, Spain

Introduction

Surfactant molecules in dilute aqueous solution self-assemble to form a variety of supra-molecules, such as micelles, vesicles and liquid crystals [1–3]. The liquid crystal (or mesophase) phase has a uni, bi or three-dimensional character and liquid properties at the molecular scale. Liquid crystals can form lamellar, hexagonal, micellar cubic or bicontinuous structures, and are thermodynamically stable and generally anisotropic. Liquid crystal systems are important not only in terms of viscosity, but also in the stabilization of foams and emulsions, and in detergency, lubrication, and other applications [4, 5]. Emulsification properties are related to the hydrophile–lipophile balance (HLB) which can predict the expected type of emulsion [5, 6].

The demand for chemical products has increased dramatically in recent years, especially for surfactants routinely used in daily life. Therefore, the use of biocompatible surfactants with low toxicity profiles is imperative. From an ecological and economical point of view, the sodium salts of sulfo fatty acid methyl esters (MES) are an alluring class of surfactants. MES is

produced using abundant and renewable natural fats and oils [7]. They are widely used in the chemical industry because of their excellent surface activity, stability toward hard water, strong detergent power [8], and self-assembly behavior [9]. In contrast to common commercial anionic surfactants based on petrochemicals, MES are environmentally benign.

The phase behavior of MES in aqueous solution has been reported by Schambil and Schwuger [10] who observed the transition to the liquid crystalline phase takes place at higher temperatures for methyl laurate and methyl palmitate as the surfactant concentration increases. In addition, Fujiwara *et al.* [11] investigated the hygroscopic and dehumidifying behavior, phase transition and hydration of the solid crystalline states and constructed a concentration temperature phase diagram for the water/α-sulfonated palmitic acid methyl ester sodium salt system that revealed the aggregation states. The influence of temperature and humidity on the crystalline structures and their impact on the mechanical characteristics of MES powder was reported by Watanabe *et al.* [12]. Lim and Ramle studied the interfacial behavior of different alkyl chain lengths at the water-MES interface [13]. MES has garnered significant attention in both scientific research and industrial applications. Several studies have focused on the use of methyl ester sulfonates as emulsifying agents to improve the storage stability of asphalt and asphalt-latex emulsions [14, 15]. They are also used as solvent replacements for aromatic hydrocarbon solvents in emulsifiable concentrate formulations [16].

In our previous works, we synthesized methyl ester sulfonates (ϕ-MES) by photosulfochlorination of lauric and myristic acids [17], producing essentially monosulfonated compounds that were referred to as sodium sulfo lauryl methyl esters (SLME) and sodium sulfo myristyl methyl esters (SMME). The resulting methyl ester sulfonates were obtained as a lightly colored powder, thereby eliminating the bleaching step. The chemical composition of these surfactants was determined, and their structures were characterized by Fourier transform infrared spectroscopy (FTIR), liquid chromatography-electrospray ionization tandem mass spectrometry and proton nuclear magnetic resonance (^{1}H-NMR). The results showed that the alpha position is not substituted and that the sulfonate group is randomly distributed along the alkyl chain, hence their name, ϕ-MES. This class of compounds has been obtained by another process cited in the literature, namely sulfoxidation using SO_2, O_2 and UV light [18]. The physicochemical properties of ϕ-MES include good surface properties and better foaming ability than that for sodium dodecyl sulfate (SDS). ϕ-MES can be used in the formulation of highly active care products. In order to valorize vegetable products by converting them into fatty acid esters by transesterification, another series of ϕ-MES surfactants were synthesized by photosulfochlorination of fatty acid esters.

This work reports the structure of ϕ-MES surfactant assemblies using polarized optical microscopy (POM) at different temperatures in conjunction with small-angle X-ray scattering (SAXS) at 25 °C, along with the effect of temperature (heating/cooling) and hydration on these structures. Geometric parameters are determined in order to deduce the aggregate structure and the conformation of the hydrocarbon chain. The emulsification properties were also studied using polarized optical microscopy and compared with those of sodium dodecyl sulfate (SDS). The results obtained are compared to the hydrophilic lipophilic balance values (HLB).

Experimental Section

Materials

Sodium dodecyl sulfate was obtained from Sigma-Aldrich (> 98.5% pure), and n-decane was obtained from Merck Schuchardt (≥ 95%). Two series of ϕ-MES compounds (sodium sulfo lauryl methyl esters [SLME], sodium sulfo myristyl methyl esters [SMME] and sodium sulfo palmityl methyl esters [SPME]) were synthesized. Compounds in the first series (SLME-1, SMME-1 and SPME-1) were synthesized from fatty acids, followed by esterification using sodium methoxide in anhydrous methanol [17]. Those of the second series (SLME-2, SMME-2 and SPME-2) were prepared from fatty methyl esters obtained from the transesterification of triglycerides.

The second series of compounds, SLME-2, SMME-2 and SPME-2, were synthesized following the method described previously [17]. The synthesized surfactants were purified by recrystallization in isopropanol, in which the insoluble salts were precipitated and the ϕ-MES surfactants were extracted in the alcohol phase and obtained after evaporation. The anionic active content (sulfonates) was determined using two-phase titration. The water content and sodium chloride were determined by the loss on desiccation and the Mohr method, respectively [17].

Polarized Optical Microscopy

The liquid crystal structure of SLME-1, SMME-1, SPME-1, SLME-2, SMME-2 and SPME-2 was determined by polarizing optical microscopy (POM). POM was carried out using a Reichert Polynov 2 polarized light microscope equipped with a Linkam THMS 600 hot stage controlled by a TP94 unit. Photomicrographs were taken with a Canon

Power shot S90 wide zoom digital camera. The hydration of the surfactant was determined by placing samples between coverslips and contacting with a drop of water. This method was based on the penetration experiment [19]. For thermal studies (heating and cooling), dry samples were placed between coverslips at 25 °C, a drop of water was then added and the temperature was increased by intervals of 5 °C from 25 to 110° C. After the heating step, the sample was cooled until the initial temperature was reached. At each step, photomicrographs of the samples were taken, and those that are most relevant are presented.

Small-Angle X-Ray Scattering and Geometric Parameters

The liquid crystalline phases were investigated using SAXS measurements. Measurements were carried out using an S3-MICRO (Hecus X-Ray systems GMBH, Graz, Austria) coupled to a GENIX-Fox 3D X-ray source (Xenocs, Grenoble), which provides a detector focused X-ray beam with the Cu Kα-line (1.542 Å) with more than 97% purity and less than 0.3% Kβ. Transmitted scattering was detected using a PSD 50 Hecus with a pixel resolution of 54.2 μm and a pixel width of approximately 1 cm. The samples were loaded in quartz capillaries with a diameter of 1 mm at 25 °C, and the temperature was controlled using a Peltier TCCS-3 Hecus to within ± 0.1 °C. Two samples were prepared for each surfactant, one dry and one hydrated. The hydrated samples were prepared by adding a small amount of water to the surfactant. The scattering curves are shown as a function of the scattered vector modulus q according to [20]:

$$q = \frac{4\pi}{\lambda}\sin(\theta/2) \tag{1}$$

and the Bragg spacing (d) is obtained by:

$$d = \frac{2\pi}{q}, \tag{2}$$

where λ is the wavelength of the X-ray source (1.542 Å) and θ is the scattering angle. Using this set-up, the q range obtained was between 0.08 and 6 nm^{-1}. The SAXS patterns are shown as obtained with the smearing on the detector.

The aggregation geometry is related to geometric constraints imposed by the structure of surfactants that are the result of interactions between the amphiphiles. For this, Israelachvili *et al.* [21, 22] defined a packing parameter (p) given by the Eq. 3.

$$p = \frac{V_c}{a_0 l_{\mathrm{Cmax}}}, \tag{3}$$

where V_C is the volume of the hydrophobic group, l_{Cmax} is the fully extended chain length of the hydrophobic group and a_0 is the cross sectional area occupied by the hydrophilic head group at the micelle solution-interface. The critical length of the hydrophobic chain (l_{Cmax}) and the volume of the hydrophobic tail in the surfactant aggregate can be calculated using Tanford equations (Eqs. 4, 5).

$$l_{\mathrm{Cmax}}(\text{Å}) = 1.5 + 1.265(n_C - 1) \tag{4}$$

$$V_C(\text{Å}) = 27.4 + 26.9(n_C - 1), \tag{5}$$

where n_C is the hydrophobic chain length in the surfactant aggregate [1, 21–25]. The area per molecule in dry lamellar structures is calculated by formula (6) where V_t is the theoretical total molecular volume and d is the Bragg distance of the first maximum [20].

$$A(\text{Å}) = \frac{2V_t}{d} \tag{6}$$

The hydrophobic (l_C) and hydrophilic lengths (l_h) are defined as the ratio of the respective hydrophobic or hydrophilic volumes to the area per molecule [26].

$$l_C(\text{Å}) = \frac{V_C}{A}, \tag{7}$$

$$l_h(\text{Å}) = \frac{V_h}{A}, \tag{8}$$

The geometric parameters for surfactant aggregation were determined based on calculated values of the maximum hydrophobic length and hydrophobic volume using Tanford equations and experimental data obtained from SAXS measurements of the area per molecule (A).

Emulsifying Properties

The emulsifying properties were measured by dissolving the surfactants in water and then adding oil [27–29]. Emulsions were prepared by adding 3 ml of oil (n-decane) to 3 ml aqueous solutions containing 30 mg of studied surfactants. Samples were shaken using a vortex mixer (VELP Scientifica-40HTZ) for 5 min at 25 °C. The mixture was poured into a 10 ml measuring cylinder with a cover. The volume of water or n-decane drained from the emulsion was measured after standing for 1 h, 48 h and 2 weeks at 25 °C. The emulsion stability was expressed as:

$$\frac{(\text{initial volume} - \text{drainage volume})}{\text{initial volume}} \times 100. \tag{9}$$

The emulsions obtained were observed using a microscope (Reichert Polynov 2). A small amount of the drained volume of emulsion was withdrawn by a micropipette and placed on a microscope glass slide, which was placed on the stage of the microscope in order to obtain photomicrographs. The dimension of the droplet along with the type of emulsion were determined by microscopic

examination in conjunction with Leica Image Manager IM500 software.

Results and Discussion

Characterization of Synthesized Compounds

The chemical structures of the two groups of ϕ-MES compounds were confirmed by FTIR, LC–MS/MS and ^{1}H-NMR. The results were in good agreement with the results reported in [17]. The chemical composition of the compounds was determined on the basis of their anionic active content (sulfonates), water content and sodium chloride. Results are shown in Table 1. ϕ-MES contains the monosodium salt (Fig. 1a) and the disodium salt (Fig. 1b). The results obtained indicate that the fatty acids are converted into the corresponding sulfonates, which contain a high percentage of monosodium sulfo fatty methyl esters (Fig. 1a) and a low percentage of disodium sulfo fatty acids (Fig. 1b). The remaining 5–10% of material is mainly free fatty acids and free fatty methyl esters.

Texture of Liquid Crystal Samples by Polarizing Optical Microscope

A phase penetration experiment was carried out initially to provide a qualitative survey of the liquid crystals. At room temperature, dry samples exhibited birefringent texture under polarized light microscopy, indicating the presence of liquid crystalline structures. All samples (Fig. 2) before heating appeared to be mostly ribbon-like fibers with a lamellar organization and non-defined birefringent areas.

In order to define the liquid crystal structure formed by these ϕ-MES surfactants, the temperature of the samples was varied from 25 to 110 °C. At 25 °C, the samples were dry, and they were hydrated by adding a drop of water, leading to the formation of different structures. It should be noted that increasing the temperature causes the evaporation of water. Different textures such as lamellar or hexagonal structures or a transition between these architectures were observed with increases in temperature, depending on the temperature and the time of sample hydration. Cooling and heating processes also affect the

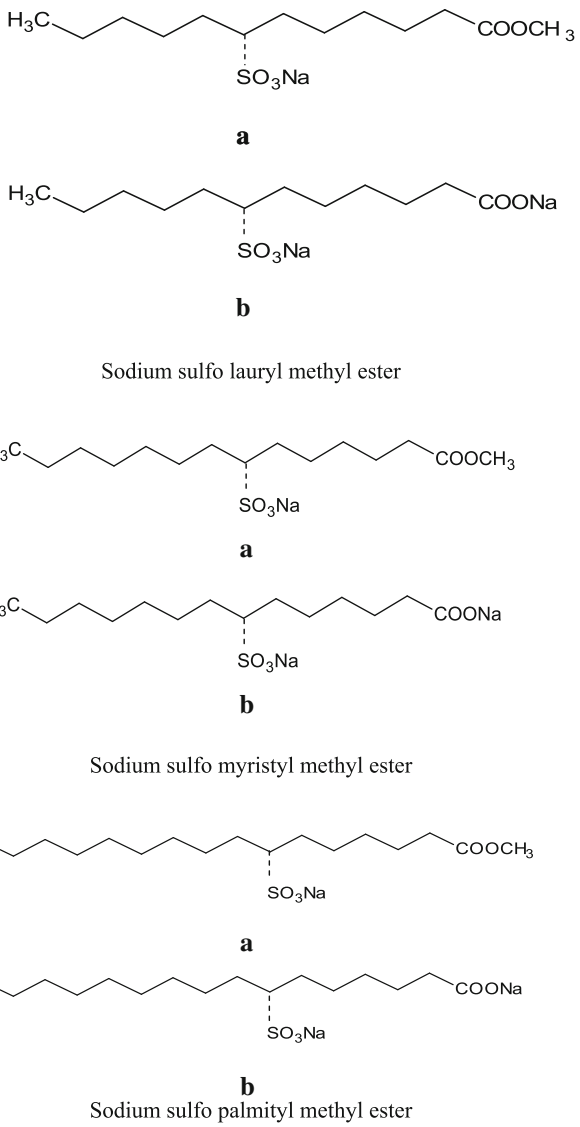

Fig. 1 Structure of the obtained compounds. **a** Mono-salts. **b** Di-salts

Table 1 Chemical composition of synthesized compounds

Compounds	Anionic active content (wt%)		wt% of water	NaCl (wt%)
	Monosodium salt	Disodium salt		
SLME-1	68.90	7.25	7.25	6.82
SMME-1	75.78	9.26	7.56	–
SPME-1	78.55	9.58	4.30	–
SLME-2	62.62	6.54	9.75	–
SMME-2	73.72	9.97	10.33	01.55
SPME-2	82.11	8.19	7.94	–

Compositions containing less than 1.5 wt% NaCl are not listed in the table

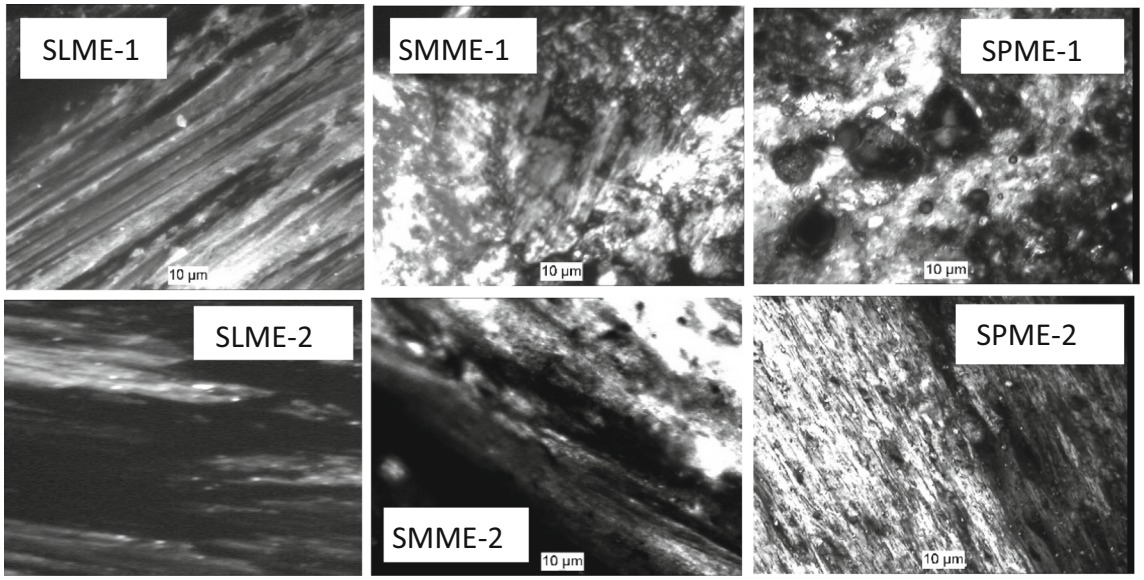

Fig. 2 Representative optical polarizing micrographs exhibited by dry samples of SLME-1, SMME-1, SPME-1, SLME-2, SMME-2, SPME-2 at 25 °C

sample structure. Micrographs corresponding to the observed textures are given in Fig. 3a, b.

Sample SLME-1 Micrographs in Fig. 3a. The hydrated sample exhibits a fan- or sheet-like shape at 25 °C, which correspond to a hexagonal phase. This structure appears after 15 min, which suggests that time is required for the equilibration of water diffusion on the surfactant sample and its hydration. After 1 h, it is unchanged, and when the temperature is increased to 80 °C, a phase transition to a lamellar structure occurs. Similar behavior is observed when the sample was heated to 110 °C and subsequently cooled to 25 °C. After a heating–cooling cycle, the lamellar structure remains unchanged after 12 and 24 h.

Sample SMME-1 Micrographs in Fig. 3a. At 25 °C, only hydrated solid was observed. A hexagonal phase emerges upon increasing the temperature to 80 °C. After cooling the hexagonal phase to 25 °C, the structure becomes undefined.

Sample SPME-1 Micrographs in Fig. 3a. A transition phase from hexagonal (at 60 °C) to lamellar structure (at 80 °C) was observed upon raising the temperature. After heating and subsequent cooling to 25 °C, the hexagonal texture is restored.

Sample SLME-2 Micrographs in Fig. 3b. The POM photos suggest the formation of a lamellar phase which remains unchanged as a function of time and increasing temperature.

Sample SMME-2 Micrographs in Fig. 3b. The micrographs show that the structure changes from lamellar to hexagonal when the sample is sufficiently hydrated and when the temperature is increased to 45 and 65 °C. At 110 °C, the hexagonal phase emerges, which undergoes a transition to the lamellar phase when the sample is cooled for 12 h.

Sample SPME-2 Micrographs in Fig. 3b. Photos of the polarizing textures show the lamellar phase at 25 °C, which changes to the hexagonal phase when the sample is hydrated and heated to 40 °C. No further change is observed up to 80 °C. Upon heating the sample to 110 °C, cooling it to 25 °C, and allowing it to sit for 12 h, a lamellar structure is observed.

Investigation of Liquid Crystals by SAXS

The small-angle X-ray technique was used to resolve periodic structures in these surfactants. The arrangements of aggregates are reflected by the relative peak intensities. Lamellar (flat micelles), two-dimensional hexagonal (cylindrical micelles) or cubic phase structures (closed micelles or bicontinuous) may be encountered [30, 31]. Structural information is directly obtained for the position of the SAXS reflections [31, 32]. On the basis of literature [33–35], when the positions of the peaks should obey to the relationships 1:2:3, equidistant spaced reflections are indicative of lamellar and double lamellar structures, and when the number of Bragg peaks are in the ratio $1:3^{1/2}:2:7^{1/2}:3$, it is the hexagonal structure. The cubic structure is characterized by 1: $(2)^{1/2}$: $(4)^{1/2}$: $(6)^{1/2}$: $(8)^{1/2}$ [36–38].

Figure 4 shows the SAXS patterns of all surfactants in the dry and hydrated state at 25 °C. They exhibit several characteristic peaks which enable unambiguous identification of the phases. The structures were first determined by visual observation using POM. Then, SAXS measurements were performed to verify the liquid crystalline phases

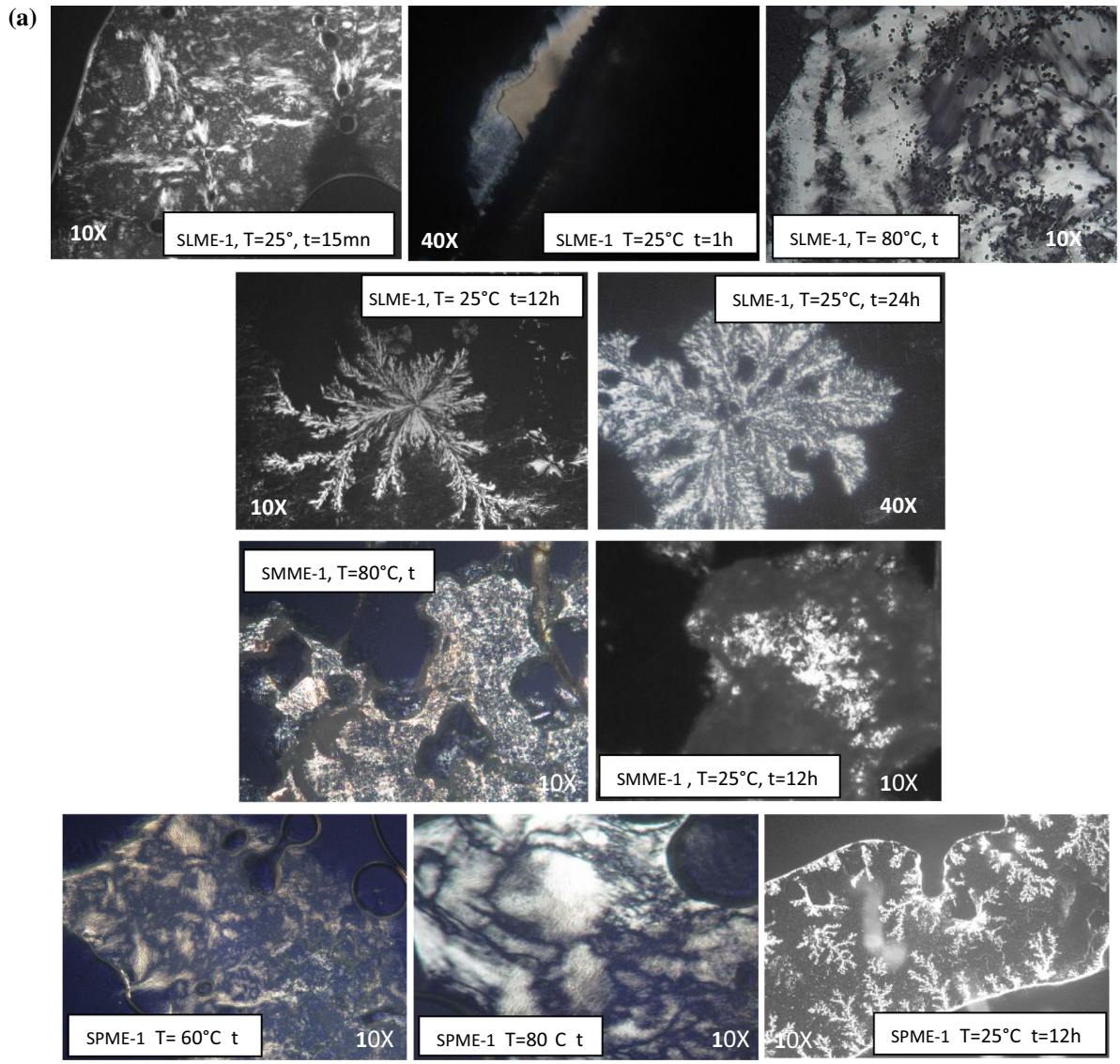

Fig. 3 **a** Images showing the evolution of recrystallization morphologies of SLME-1, SMME-1 and SPME-1 during stages of heating and subsequent cooling. t = time corresponding to a specific temperature. **b** Images showing the evolution of recrystallization morphologies of SLME-2, SMME-2 and SPME-2 during stages of heating and subsequent cooling down. t = time corresponding to a specific temperature

present in the systems. Microscopically, lamellar and hexagonal lyotropic liquid crystalline phases are clearly observed. These structures depend on temperature and the hydration time. From SAXS measurements, we observe a lamellar structure for SLME-1, SPME-1, SLME-2 and SPME-2, but a transition from lamellar to double lamellar structures is observed for SMME-1 and from double lamellar to lamellar structure for sample SPME-2 upon hydration. To confirm the liquid crystalline phases, the scattering vector modulus (q) and the interlayer spacing were measured by SAXS (Fig. 4). The Bragg spacing (d) and the theoretical and experimental extended chain length (l_{Cmax}) were determined and are presented in Table 2. The structure of the liquid crystalline phases can be interpreted from the d-spacing values of the obtained diffraction rings.

Sample SLME-1 The curve in Fig. 4 shows the intensity of SAXS from the dry and hydrated sodium lauryl methyl ester sulfonates at 25 °C. The diffraction peaks occurring at $q = 0.195$ and 0.390 Å^{-1} (see Table 2) suggest a lamellar structure for the dry and hydrated states. When the sample is incubated with water for an extended duration (24 h), it undergoes slight swelling, and a third peak that emerges within our experimental window at $q = 0.585$ Å^{-1} confirms the lamellar structure. The position of peaks corresponding to the ratio 1:2:3 confirms the lamellar phase.

Fig. 3 continued

(b)

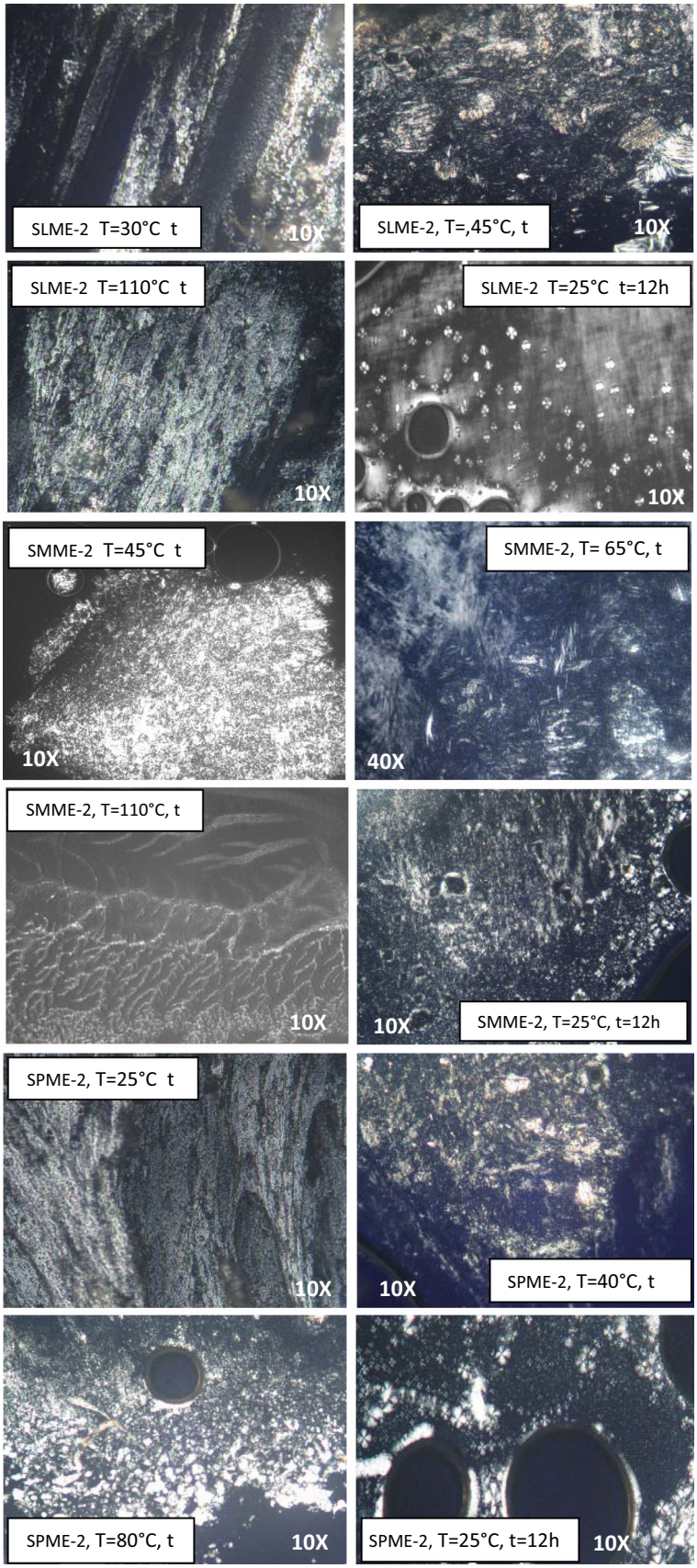

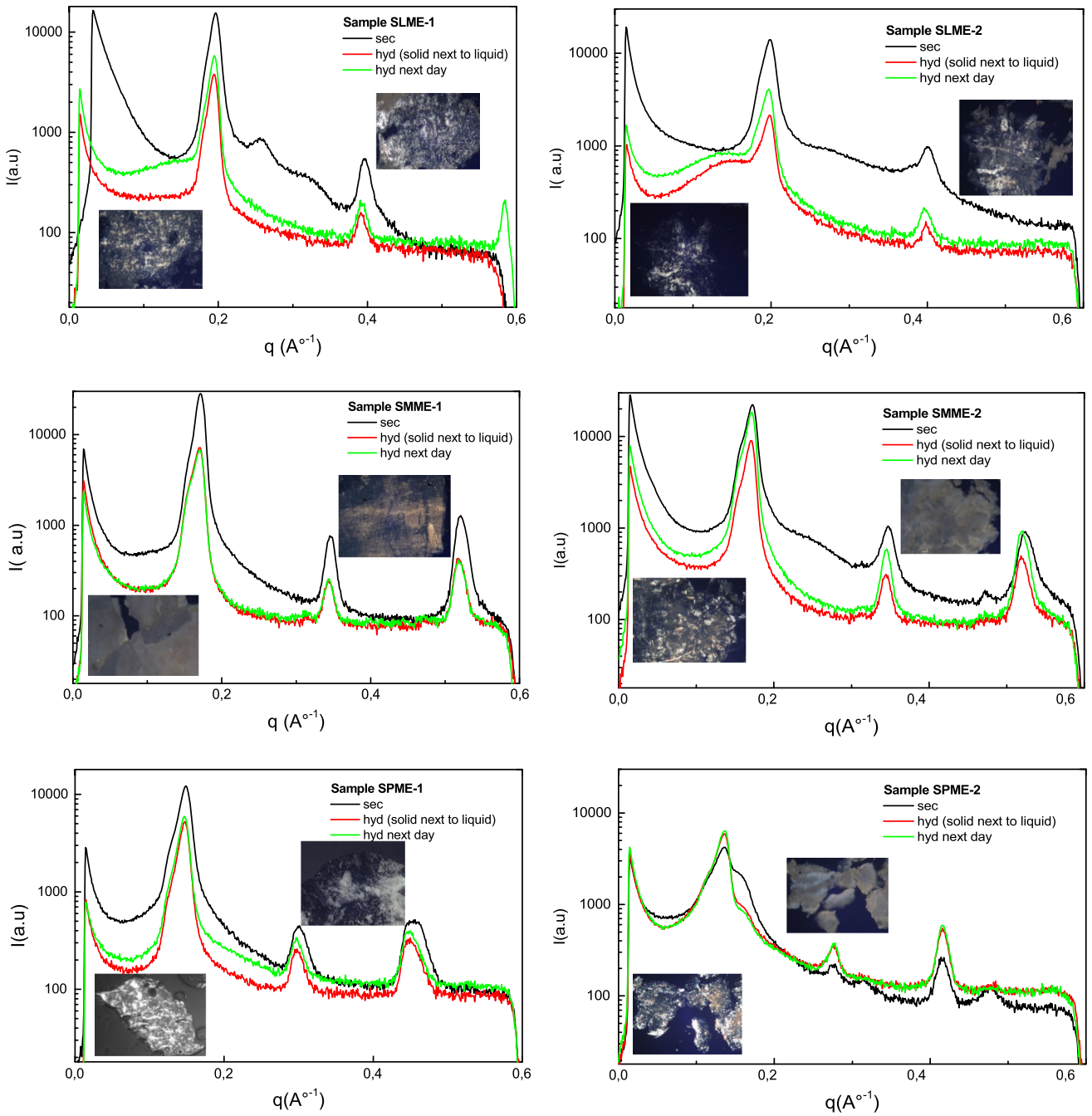

Fig. 4 The scattering profiles obtained at 25 °C. Images on the right correspond to the dry samples and those on the left to the hydrated samples

These structures in different states are very similar, and in this case, they correspond to a repeating distance of 32.20 Å.

Sample SMME-1 The SAXS diffraction patterns in Fig. 4 corresponding to the dry and hydrated sodium myristyl methyl ester sulfonates at 25 °C show three reflections occurring at $q = 0.173$; 0.345 and 0.520 $Å^{-1}$ which indicate that the dry state structure is lamellar, but in the presence of water, a new peak emerges. The reflection of this peak occurs at $q = 0.157 Å^{-1}$, which suggests the double lamellar structure. This result leads to a distance of 36.30 Å for the dry sample and a distance of 40.00–36.94 Å for the hydrated sample. SMME-1 exhibits a longer distance than the original spacing of the lamellar phase of sample SLME-1.

Sample SPME-1 The scattering profile of the dry palmityl methyl ester sulfonates in Fig. 4 shows three reflections occurring at $q = 0.150$; 0.301 and 0.445 $Å^{-1}$ that suggests a lamellar structure. This structure is the same as that observed for the hydrated sample with reflections

Table 2 Structural properties of the various samples obtained by SAXS at 25 °C

Sample abbreviations	Structure		q (Å^{-1})		d (Å)	
	Dry	With water	Dry	With water	Dry	With water
SLME-1	Lamellar	Lamellar	0.195	0.195	32.20	32.20
SLME-2	Lamellar*	Lamellar	0.197	0.197	31.87	31.87
SMME-1	Lamellar	Double lamellar	0.173	0.157	36.30	40.00
				0.170		36.94
SMME-2	Double lamellar	Lamellar	0.161	0.170	39.00	37.00
			0.169		37.15	
SPME-1	Lamellar	Lamellar	0.150	0.148	41.86	42.4
SPME-2	Lamellar*	Lamellar*	0.135	0.135	46.51	46.51
			0.153	0.159	41.04	39.49

*In the structure next to the lamellar structure some extra peaks are present

occurring at $q = 0.148$; 0.295; 0.444 Å^{-1}. Table 2 shows that the distance is even longer for SPME-1; it is 41.86–42.2 Å for the dry and hydrated samples, respectively, which suggests that increasing the number of carbon atoms occurs with a concomitant increase of the distance for the same series of surfactants.

Sample SLME-2 The SAXS curve in Fig. 4 confirms the lamellar structure observed by polarizing optical microscopy and shows some peaks and the values of reflections at $q = 0.197$ and 0.401 Å^{-1}, suggesting a lamellar structure for the dry sample. In the presence of water, the reflections appear at $q = 0.197$ and 0.388 Å^{-1} indicating that the lamellar structure is unchanged. The calculated repeating distance of 40.00 Å is unchanged.

Sample SMME-2 The SAXS results in Fig. 4 exhibit reflections at $q = 0.169$; 0.347; 0.524 Å^{-1} and the appearance of a peak at $q = 0.161$ Å^{-1}, suggesting a double lamellar structure. When the sample is hydrated, the reflections appear at $q = 0.170$; 0.345; 0.518 Å^{-1}, indicating that the structure has changed. Hydration gives rise to a transition from the double lamellar to a lamellar structure. This result gives a repeating distance of 39.00–37.15 Å and 37 Å for the dry and hydrated states.

Sample SPME-2 The microscopic observations are in accordance with the SAXS curve in Fig. 4, which shows the appearance of three reflections. These reflections occurring at $q = 0.135$; 0.276 and 0.415 Å^{-1} suggest a lamellar structure for the dry and hydrated state. In addition, some extra peaks were observed next to the lamellar structure at $q = 0.153$ and 0.159 Å^{-1} for the dry and hydrated state, respectively. Table 2 shows that the distance is even longer for SLME-2.

The structures of the surfactants synthesized from fatty acids (SLME-1, SMME-1 and SPME-1) and those synthesized from fatty acid esters (SLME-2 SMME-2 and SPME-2) exhibit differences that may be due to their composition. As explained previously, the methyl ester sulfonates contain different proportions of the active monosalt and the disodium salt whose content is lower than 10%. This difference in chemical composition impacts the water solubility of the surfactants, and thus their hydration. Furthermore, the composition (surfactant/water) has an influence on the structure. Some surfactants have pseudo-polymorph structures which are transformed to hydrated states that are affected by the temperature and humidity [39]. Abe *et al.* [40] reported that ϕ-MES forms some hydrate crystals as evidenced by X-ray diffraction. Fujiwara *et al.* [11] obtained lamellar liquid crystals at 80 °C for C16MES, which has 3.5 wt% moisture content. Watanabe *et al.* [12] found that the mixture of C16MES/C18MES (3.5 wt% moisture content) in an 85:15 ratio by volume at 20 °C formed hexagonal lattice and lamellar structures at 80 °C. The same results are obtained for SPME-1 and SPME-2 with 4.30 and 7.94 wt % moisture content, respectively, at 25 °C. In addition, Watanabe *et al.* [12] reported that the crystalline structure of ϕ-MES was transformed from a metastable crystal to a mixture of anhydrous crystals and dehydrated crystals due to melt-mediated crystallization.

The hexagonal phase shown in Fig. 3a, b can be explained by the increase in temperature, which usually leads to an increase in the surfactant monomer concentration. This reflects the increased solubility of the monomeric surfactant [6] and the greater thermal mobility and solubility of the hydrophobic tail. However, the higher temperature reduces the degree of hydration, and facilitates the formation of the lamellar aggregates. These results are in accordance with literature data which report that the crystalline structure of ϕ-MES changes as a function of temperature [12]. Schambil and Schwuger [10] showed that methyl laurate and methyl palmitate transition occurs from an isotropic solution to a hexagonal liquid crystalline phase at higher temperatures. The cooling/heating cycle is also necessary to form certain liquid crystals. The compounds

exhibit phase transitions upon hydration followed by heating, which enables greater penetration by water; however, at elevated temperatures, the water evaporates. Cooling also affects the structure of phases that appear as lamellar and transition to hexagonal, as well as the reverse process. These structures are easier to define after an equilibrium period. These results are consistent with the phases identified after cooling [41, 42]. Cooling may change the normal (isotropic) liquid to anisotropic liquid (nematic liquid crystal). Further cooling may cause the anisotropic liquid to change into the lamellar structure; this is the smectic A phase. On further cooling, the molecules may tend to tilt a little giving rise to the smectic C phase. In other substances, further cooling the smectic A phase results in the breaking up of the layers into hexagons, which constitutes the smectic B_{Hex} phase [43].

The Krafft temperatures of the products were determined according to the procedure described in Ref. [17], and were 25.0; 28.0; 33.9; 25.6; 29.0 and 33.3 °C for SLME-1, SMME-1, SPME-1, SLME-1, SMME-1 and SPME-1, respectively. This shows that the solubility decreases with increasing chain length, which makes hydration more difficult. These results are in accordance with the work of Okano *et al*. [43] who found that almost all sodium α-sulfonated fatty acid methyl esters studied exhibited relatively high Krafft points and did not dissolve in water at room temperature, leading the authors to suggest that sodium α-sulfonated fatty acid esters form bilayer membranes, like vesicles or lamellar liquid crystals, rather than micelles in water.

Dimension Packing Parameters

The geometric packing parameters obtained by SAXS are given in Table 3, which also includes the theoretical volume of the molecule (V_t), the maximum hydrophobic length (l_{Cmax}), the hydrophobic volume (V_C) according to Tanford equations [1], the hydrophilic volume (V_h) and the hydrophilic length.

The theoretical hydrophobic length corresponds to $[1.265 \times (n_C - 1)]$ when the length of the chain is completely extended and the experimental hydrophobic length value is obtained by (d/2). The hydrophobic lengths are close to the maximum expected values, and the ratio of the theoretical and experimental values of all samples are around 0.9, which suggests that surfactants are tilted with an angle of $\theta = 25°$. The area per molecule, calculated by formula (6), shows that the area per molecule decreases upon increasing the number of carbon atoms, which is in agreement with the literature [5]. Myers [6] reported that the molecules of surfactants were slightly tilted, and this may lead to an increase in the effectiveness of adsorption as the length of the alkyl chain is increased. This effect is not surprising when one considers that a greater dispersion force interaction resulting from a larger alkyl group can lead to greater lateral interactions among surfactant molecules, enabling a greater packing density for longer chains.

Emulsion Stability

Emulsions were prepared using a mixture of water and n-decane in the presence of the synthesized surfactants (SLME-1, SMME-1, SPME-1, SLME-2, SMME-2 and SPME-2) and compared to the anionic surfactant, SDS. Table 4 summarizes the emulsion stabilities of the synthetic surfactants and SDS. After vigorous shaking, the surfactants formed emulsions, which were stable after 2 weeks and were around 60% for all surfactants, with the exception of SPME-2, which is comparable to that of SDS. The instability of SPME-2 can be explained on the basis of its composition (mono and di-salts). Hoefer *et al*. [44] reported that among MES surfactants used in the production of synthetic materials, such as the polymerization of ethylenically unsaturated monomers, emulsifiers composed of a 22:88 mixture of disodium sulfolaurate and sodium sulfo methyl laurate formed emulsions that were more stable than emulsions obtained from *n*-dodecylbenzenesulfonate. In the present study, the surfactants were first

Table 3 Some geometric parameters of samples

Sample abbreviations	l_{Cmax} (Å)	l_C (Å)	A (Å^2)	V_C (Å^3)	V_h (Å^3)	l_h (Å)
SLME-1	16.68 (33.36)*	16.10	34.62	350.20	173.80	05.02
SMME-1	19.21 (38.42)*	18.15	31.46	404.00	167.00	05.30
SPME-1	21.74 (43.48)*	20.73	30.44	457.80	160.20	05.26
SLME-2	16.68 (33.36)*	15.93	34.61	350.20	173.80	05.02
SMME-2	19.21 (38.42)*	19.75	32.26	404.00	167.00	05.17
SPME-2	21.74 (43.48)*	23.6	30.55	457.80	160.20	05.24

*Refers to two chains, l_{Cmax} maximum hydrophobic length, V_C volume of hydrophobic part of surfactant are calculated from Tanford equations, l_C experimental hydrophobic length, V_h volume of hydrophilic part of surfactant, l_h hydrophilic length

Table 4 Emulsifying performance of samples

Sample abbreviations	Time (h)	Emulsion stability (%)
SLME-1	1	83.33
	48	66.66
	336	60.00
SMME-1	1	71.01
	48	65.21
	336	65.21
SPME-1	1	72.22
	48	70.45
	336	65.90
SLME-2	1	81.81
	48	63.63
	336	56.36
SMME-2	1	86.86
	48	79.79
	336	70.20
SPME-2	1	56.89
	48	52.06
	336	50.00
SDS	1	83.84
	48	62.68
	336	61.22

dissolved in water and then oil was added, thus favoring the formation of O/W emulsions as reported in the literature [45, 46]. During the emulsification, the emulsifiers adsorb at the oil–water interface, thereby reducing the interfacial tension while providing steric and electrostatic stabilization of the droplets. The emulsification properties and the type of emulsion may change with as a function of the structure of the emulsifier when the amounts and volumes of both phases are the same. It was reported by Dong *et al.* [47] that when hydrophilic emulsifiers preferably remain in the aqueous phase, O/W emulsions will be formed. However when hydrophobic emulsifiers are used, stable W/O emulsions will be produced. As expected, O/W emulsions are formed when ϕ-MES is used.

Differences in the refractive index between dispersed and continuous media confirmed that O/W dispersions were formed [46]. These surfactants are water soluble and form micelles and liquid crystals in aqueous solutions that can favor the formation of O/W dispersions as observed by optical microscopy. Bancroft's rule states that the formation of more preferable emulsion types will occur in continuous phases where self-aggregation of the surfactant takes place [5, 45, 46]. Thus, in water, ϕ-MES surfactants will tend to give O/W emulsions. These results are in agreement with the HLB values obtained in a previous study [17], where the method of determination was

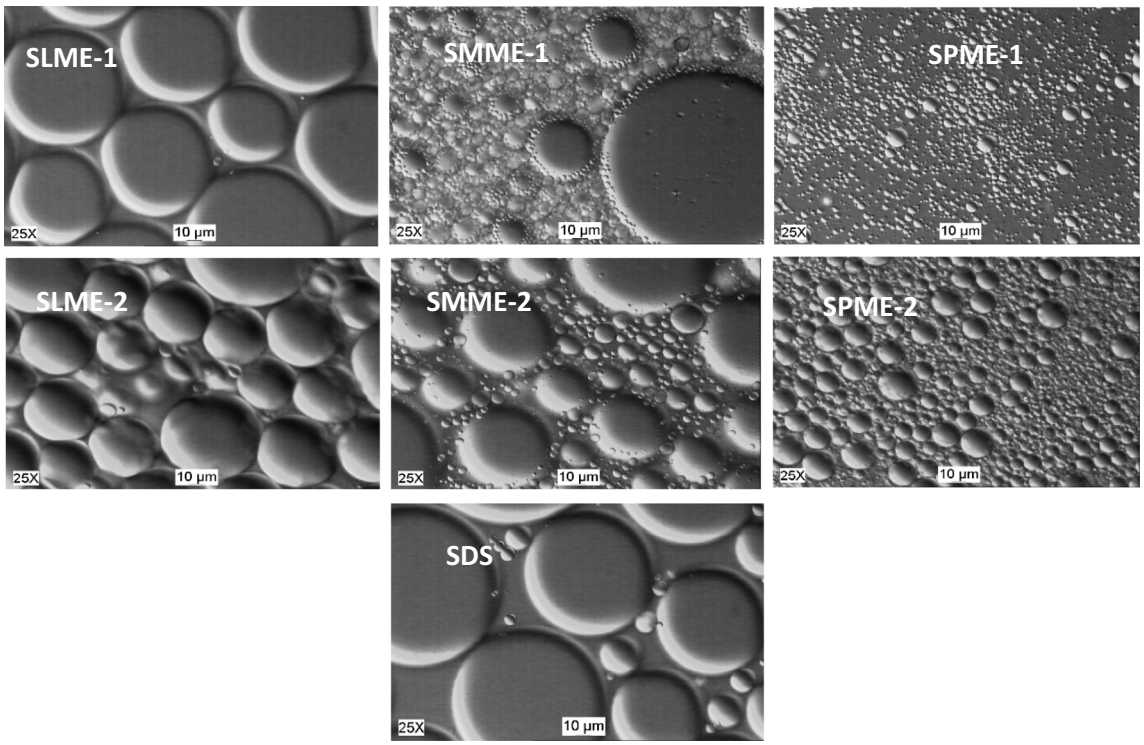

Fig. 5 Photomicrographs of emulsions for samples and SDS

described for SLME-1 (HLB = 14.37) and SMME-1 (HLB = 13.11) along with SPME-1 (HLB = 13.31), SLME-2 (HLB = 14.54), SMME-2 (HLB = 14.69) and SPME-2 (HLB = 13.79). The results confirm the formation of an 'oil-in-water' emulsion, and show that the synthesized surfactants and SDS exhibit a hydrophilic tendency. Polarized light images (Fig. 5) show that SLME-1 forms an emulsion with drops as large as those formed by SDS. In the case of SPME-1 and SPME-2, the sizes are very polydisperse, and the drops formed by SPME-2 are larger than those of SPME-1. It has been reported that the length of the hydrophilic chain of the surfactant has a certain influence on the mean diameter of the dispersed phase of the emulsion. In fact, the mean diameter of the dispersed phase of the emulsion decreases significantly when the chain length increases, which renders the emulsion unstable [48].

Conclusion

In the present paper, we have investigated the self-aggregation and emulsifying properties of ϕ-MES surfactants. An understanding of the crystalline structures of this class of surfactants, and the effect of parameters such as temperature and hydration, is important for their application in detergents. The POM study revealed the birefringent structures of the studied surfactants, and SAXS results obtained at room temperature demonstrated the presence of crystalline phases. SAXS patterns showed the presence of lamellar phases for SLME-1, SPME-1, SLME-2 and SPME-2, and double lamellar phases for SMME-1 and SMME-2. Polarizing optical microscopy revealed that heating and cooling affected the structure of the liquid crystal. Hydration was also found to play an important role in defining the structure of the surfactants. In the majority of cases, an equilibrium state was required for the organization of the surfactants in a regular packing motif. At higher temperatures, POM showed that the degree of hydration was reduced, and the lamellar aggregate was formed and the hexagonal phase appeared with an increase in temperature. With respect to the results of SAXS, the Bragg distances were calculated and were found to decrease upon increasing the carbon number from 13 to 17 for each series of surfactants. The values of repeating distance (d) suggests that the chain structure of these surfactants is tilted. Surfactants with 15 carbon atoms, such as SMME-1 and SMME-2, formed the most stable emulsions. POMs showed that increasing the number of carbon atoms (from 13 to 17 carbons) was accompanied by a decrease in the size of the emulsions. Based on the images of the polarizing optical microscopy and the obtained HLB values, ϕ-MES surfactants formed O/W emulsions and may hold potential for use in detergent applications.

Acknowledgements This research was supported by the Department of Surfactant Technology, Institute of Advanced Chemistry of Catalonia-Spanish Council for Scientific Research, under project MINECO-CTQ 2013-41514-P. J. Caelles from the SAXS- WAXS service at IQAC is kindly acknowledged for his help with SAXS measurements.

References

1. Tanford C. The hydrophobic effect: formation of micelles and biological membranes. Chapter 12, Motility and Order. 2nd ed. New York: Wiley; 1980. p. 128–38.
2. Lindman B, Wennerström H. Micelles. Amphiphile aggregation in aqueous solution. Top Curr Chem. 1980;87:1–87.
3. Degiorgio V, Corti M. Physics of amphiphiles-micelles, vesicles, and microemulsions. Amsterdam: Noth-Holland; 1985. p. 121–51.
4. Boschkova K, Kronberg B, Stalgren JJR, Persson K, Salageon MR. Lubrication in aqueous solutions using cationic surfactants—a study of static and dynamic forces. Langmuir. 2002;18:1680–7.
5. Rosen MJ. Surfactants and interfacial phenomena. 3rd ed. New York: Wiley; 2004. p. 107–313.
6. Myers D. Surfactant science and technology. 3rd ed. New Jersey: Wiley; 2006. p. 281–312.
7. Chupa J, Misner S, Sachdev A, Wisnelwky P, Smith GA. Saop, fatty acids, and synthetic detergents. In: Kent JA, editor. Handbook of industrial chemistry and biotechnology. 12th ed. USA: Springer; 2012. p. 1431–72.
8. Cohen L, Trujillo F. Performance of sulfoxylated fatty acid methyl esters. J Surfactants Deterg. 1999;2:363–5.
9. Yueming J, Senlin T, Jiali G, Xiao R, Xinyan L, Shumei G. Synthesis, characterization and exploratory application of anionic surfactant fatty acid methyl ester sulfonate from waste cooking oil. J Surfactants Deterg. 2016;19:467–75.
10. Schambil F, Schwuger MJ. Physico-chemical properties of alpha sulpho fatty acid methyl esters and alpha sulpho fatty acid methyl esters di-salts. Tenside Surf Det. 1990;27:380–5.
11. Fujiwara M, Okano T, Amano H, Asano H, Ohbu K. Phase diagram of α-sulfonated palmitic acid methyl ester sodium salt-water system. Langmuir. 1997;13:3345–8.
12. Watanabe H, Morigaki A, Kaneko Y, Tobori N. Effects of temperature and humidity history on brittlness of α- sulfonated fatty acid methyl ester salt crystals. J Oleo Sci. 2016;65:143–50.
13. Lim WL, Ramle RA. The behavior of methyl esters sulphonate at the water-oil interface: straight-chained methyl ester from lauryl to stearyl as an oil phase. J Dispers Sci Technol. 2009;30:131–6.
14. Holmberg K. Novel surfactants: preparation applications and biodegradability, vol. 114. 2nd ed. USA: Mercel Dekker; 2005. p. 109–10.
15. Karsa DR, Porter MR. Biodegradability of surfactants. 2nd ed. London: Chapman and Hall; 1994. p. 257.
16. Nalewaja JD, Robert Goss G, Scott Tann R. Pesticide formulations and application systems. ASTM USA. 1998;18:194.
17. Asselah A, Tazerouti A. Photosulfochlorination synthesis and physicochemical properties of methyl ester sulfonates derived from lauric and myristic acids. J Surfactants Deterg. 2014;17:1151–60.
18. Cohen L, Trujillo F. Synthesis, characterization, and surface properties of sulfoxylated methyl esters. J Surfactants Deterg. 1998;1:335–41.

19. Lawrence ASC. Polar interactions in detergency. In: Durham K, editor. Surface activity and detergency. London: Macmillan; 1961. p. 158.
20. Pinazo A, Angelet M, Pons R, Lozano M, Infante MR, Pérez L. Lysine-bisglycidol conjugates as novel lysine cationic surfactants. Langmuir. 2009;25:7803–14.
21. Israelachvili JN, Mitchell DJ, Ninham BW. Refinement of the fluid-mosaic model of membrane structure. Biochim Biophys Acta. 1977;470:185–201.
22. Israelachvili JN, Mitchell DJ, Ninham BW. Theory of self-assembly of hydrocarbon amphiphiles into micelles and bilayers. J Chem Soc Faraday Trans. 1976;72:1525–68.
23. Israelachvili JN. The sciences and applications of emulsions—an overview. Colloids Surf, A. 1993;91:1–8.
24. Tartar HV. A theory of the structure of the micelles of normal paraffin-chain salts in aqueous solution. J Phys Chem. 1955;59:1195–9.
25. Small DM. The physical chemistry of lipids: handbook of lipid research, vol. 4. New York: Plenum; 1986. p. 97–232.
26. Pinazo A, Perez L, Lozano M, Angelet M, Infante MR, Vinardell MP, Pons R. Aggregation properties of diacyl lysine surfactants derivatives: hydrophobic chain length and counterion effect. J Phys Chem B. 2008;112:8578–85.
27. Infante MR, Moses V. Synthesis and surface activity properties of hydrophobic/hydrophilic peptides. Int J Pept Protein Res. 1994;43:173–9.
28. Shimada A, Yamammoto L, Sase H, Yamazaki Y, Watanabe M, Arai S. Surface properties of enzymatically modified proteins in aqueous solution. Agric Biol Chem. 1984;48:2681–8.
29. Pons R, Erra P, Concepcion Solans. Viscoelastic properties of gel-emulsions: their relationship with structure and equilibrium properties. J Phys Chem. 1993;97:12320–4.
30. Katsaras J, Gutberlet T. Lipid bilayers: structure and interactions. Biological Physics Series. New York: Springer; 2001. p. 9–19.
31. Merta J, Torkkeli M, Ikonen T, Serimaa R, Stenius P. Structure of cationic starch (SC)/anionic surfactant complexes studied by small angle X-ray scattering (SAXS). Macromolecules. 2001;34:2927–46.
32. Brown GH, Wolken JJ. Liquid crystals and biological structures. New York: Academic Press; 1979. p. 165–7.
33. An Y, Xu J, Zhang J, Hu C, Li G, Wang Z, Wang Z, Zhang X, Zheng L. Studies on the phase properties of lyotropic liquid crystals of brij35/sodium oleate/oleic acid/water system: by means of polarizing microscope, saxs, 2H-NMR and rheological methods. Sci China Ser: Chem. 2006;49:411–22.
34. Luzzati V, Ph D, Husson F. Liquid-crystalline phases of lipid-water systems. J Cell Biol. 1962;12:207–19.
35. Alexandridis P, Olsson U, Lindman B. A record nine different phases (four cubic, two hexagonal, and one lamellar lyotropic liquid crystalline and two micellar solutions) in a ternary isothermal system of an amphiphilic block copolymer and selective solvents (water and oil). Langmuir. 1998;14:2627–38.
36. Holmberg K. Handbook of applied surface and colloid chemistry. New York: Wiley; 2001. p. 299–323.
37. Nainggolan I, Radiman S, Hamzah AS, Hashim R. Colloids Surf B. 2009;73:84–91.
38. Mezei A, Pérez L, Pinazo A, Comelles F, Infante MR, Pons R. Self-assembly of pH-sensitive cationic lysine based surfactants. Langmuir. 2012;28(49):16761–71.
39. Kekicheff P, Madelmont GC, Ollivion M. Phase diagram of sodium dodecyl sulfate-water system. J Colloid Inter Sci. 1989;131:112–32.
40. Abe Y, Harata K, Fujiwara M, Ohbu K. Intercalation of cations in crystalline anionic surfactants. J Chem Soc Perkin Trans. 1999;2:85–97.
41. Freidel G. The mesomorphic states of matter. Ann Physique. 1922;18:273–474.
42. Blinov Lev M. Structure and properties of liquid crystals, vol. 1. The Netherlands: Springer; 2011. p. 41–148.
43. Okano T, Tanabe J, Fukuda M, Tanaka M. α-sulfonated fatty acid esters: structural effects of sodium α-sulfonated fatty acid higher alcohol esters on surface-active properties and emulsification ability. J Am Oil Chem Soc. 1992;69:1.
44. Hoefer R, Bartnick B, Schmid KH and Wagemud B (1985) Ger. Patent 3,339,407 to Henkel K.-G.a.A.
45. Binks BP. Emulsions, recent advances in understanding in modern aspects of emulsion science. Cambridge: The Royal Society of Chemistry; 1998. p. 56–174.
46. Elena Bautista M, Pérez L, Teresa García M, Cuadros S, Marsal A. Valorization of tannery wastes: lipoamino acid surfactant mixtures from the protein fraction of process wastewater. Chem Eng J. 2015;262:399–408.
47. Dong X, Zhang W, Zong Q, Liu Q, He J. Physicochemical and emulsifying properties of "extended" triblock copolymers. Colloid Polym Sci. 2015;293:376. doi:10.1007/s00396-014-3420-8.
48. Bibette J, Goutayer M, Texier-Nogues I (2008) Method for preparing nano-emulsions. WO 2008104717 A2

Amel Asselah received her Ph.D in Organic Chemistry (2015) from the University of Sciences and Technology Houari Boumediene (USTHB), Algiers, Algeria. She is a teacher at the Department of Process Engineering, Faculty of Engineering Sciences (FSI), University M'Hamed Bougara (UMBB) of Boumerdes, Algeria. During her doctorate, she joined the Department of Surfactants Technology, Institute of Advanced Chemistry of Catalonia-Spanish Council for Scientific Research (CSIC-IQAC), Barcelona, Spain, on an Algerian fellowship (2014). Her research interests are in anionic surfactants, their synthesis, properties, and applications.

Aurora Pinazo received Ph.D in Biology in 1988 from the University of Barcelona. Her main areas of interest include surfactants and their physicochemical properties. She was introduced to the study of these properties in 1992 while visiting the Chemical Engineering School at Purdue University, Indiana, USA. Since 1999, she has held a Tenure research position at the Spanish Council for Scientific Research (CSIC).

Amalia Mezei studied chemistry at babes-Bolyai University, Romania. Afterwards, she specialised in physical chemistry and finished her Ph.D in colloid chemistry in 2008 at Eotvos Lorand, University of Budapest, Hungary. Between 2009 and 2010, she was post-doc at Eotvos Lorand, and from 2010 to 2014 at CSIC-IQAC, Barcelona. She is from 2014, a research scientist at Tyco Fire Protection Products in Germany.

Lourdes Pérez received her Ph.D in chemistry from the University of Barcelona in 1997. Since 2002, she has been a research scientist at the Consejo Superior de Investigaciones Scientificas, Barcelona, Spain. Her research focuses on molecular design, chemical synthesis and evaluation of biocompatible surfactants from amino acids.

Amel Tazerouti received her master's degree in organic chemistry (1988) and her Ph.D in organic chemistry (1994) from the University of Sciences and Technology Houari Boumediene (USTHB), Algiers, Algeria. During her doctorate, she joined the Department of Chemistry, Catholic University of Louvain, Belgium, on a Belgium fellowship. She is currently a Professeur and Director of the Laboratory of Applied Organic chemistry, Faculty of Chemistry, USTHB. Her main research fields are the synthesis and properties of surfactants.